Digital Discovery

ROYAL SOCIETY OF CHEMISTRY

PAPER

View Article Online
View Journal | View Issue

Cite this: *Digital Discovery*, 2025, **4**, 2521

Multireference error mitigation for quantum computation of chemistry

Hang Zou, [ab] Erika Magnusson, [a] Hampus Brunander, [a] Werner Dobrautz *[acd] and Martin Rahm [a]

Quantum error mitigation (QEM) strategies are essential for improving the precision and reliability of quantum chemistry algorithms on noisy intermediate-scale quantum devices. Reference-state error mitigation (REM) is a cost-effective chemistry-inspired QEM method that performs well for weakly correlated problems. However, the effectiveness of REM is often limited when applied to strongly correlated systems. Here, we introduce multireference-state error mitigation (MREM), an extension of REM that systematically captures quantum hardware noise in strongly correlated ground states by utilizing multireference states. A pivotal aspect of MREM is using Givens rotations to efficiently construct quantum circuits to generate multireference states. To strike a balance between circuit expressivity and noise sensitivity, we employ compact wavefunctions composed of a few dominant Slater determinants. These truncated multireference states, engineered to exhibit substantial overlap with the target ground state, can effectively enhance error mitigation in variational quantum eigensolver experiments. We demonstrate the effectiveness of MREM through comprehensive simulations of molecular systems H_2O, N_2, and F_2, underscoring its ability to realize significant improvements in computational accuracy compared to the original REM method. MREM broadens the scope of error mitigation to encompass a wider variety of molecular systems, including those exhibiting pronounced electron correlation.

Received 16th May 2025
Accepted 28th July 2025

DOI: 10.1039/d5dd00202h

rsc.li/digitaldiscovery

I. Introduction

Quantum computers hold considerable promise for solving computationally infeasible problems for classical computers.[1–3] They have the potential to speed up the simulation of quantum systems and to offer exponential memory storage capabilities.[4–6] Quantum chemistry, in particular, is expected to gain potential long-term benefits from advances in quantum computing.[7–11] However, current noisy intermediate-scale quantum (NISQ) devices[12] are susceptible to noise, which can result in loss of coherence during computation, thus undermining potential quantum advantages.[13,14] Even for NISQ algorithms featuring shallow circuits, such as the variational quantum eigensolver (VQE)[15,16] or variational quantum imaginary time evolution (VarQITE),[17–19] errors inevitably accumulate during computation, leading to unreliable results. The current number and fidelity of physical qubits do not meet the demands of fault-tolerant quantum computing utilizing quantum error-correcting codes.[20–23] Therefore, pursuing alternative approaches to achieve meaningful results and accelerate the practical application of NISQ devices is crucial.

Research in quantum error mitigation (QEM) shifts the focus from hardware resources to sophisticated information processing techniques.[24–43] QEM typically involves executing an ensemble of noisy circuits multiple times or making moderate circuit modifications, followed by post-processing the noisy data to infer ideal computational results. Numerous QEM methods have been proposed to improve the quality of results calculated with NISQ hardware, including error extrapolation,[26,35] probabilistic error cancellation,[26,36] virtual distillation,[30,37] measurement error mitigation,[32,33,41] symmetry constraints,[29,40] subspace expansions,[34,39] learning-based methods,[31,38,42,43] and reference-state error mitigation (REM).[28] The cost of using a QEM strategy is paid in additional sampling costs, which primarily determine the feasibility and scalability of a QEM protocol. Many QEM methods incur exponential sampling overhead as circuit depth and qubit count increase.

Several universal frameworks have been proposed to evaluate the minimum sampling requirements of general QEM protocols, highlighting the inherent exponential challenges to QEM scalability.[44–47] These frameworks provide task-agnostic

[a]*Department of Chemistry and Chemical Engineering, Chalmers University of Technology, 41296 Gothenburg, Sweden. E-mail: werner.dobrautz@gmail.com; martin.rahm@chalmers.se*

[b]*Department of Computer Science and Engineering, Chalmers University of Technology and University of Gothenburg, 41296 Gothenburg, Sweden*

[c]*Center for Advanced Systems Understanding, Helmholtz-Zentrum Dresden-Rossendorf, Germany*

[d]*Center for Scalable Data Analytics and Artificial Intelligence Dresden/Leipzig, TU Dresden, Germany*

guarantees, assuming no prior knowledge about the problem structure. However, in specific domains such as quantum chemistry, physically motivated assumptions—for example, the availability of a good trial wavefunction or an approximate model of the target state—can often be leveraged to design more efficient QEM strategies, significantly reducing the sampling cost in practice.

The REM method, described in detail in Section II B, leverages chemical insight to provide a low-complexity error mitigation approach, requiring at most one additional algorithm, *e.g.* VQE/VarQITE iteration.[28,48] The idea of REM is to mitigate the energy error of a noisy target state measured on a quantum device by first quantifying the effect of noise on a close-lying reference state. The reference state, often also set to be the initial state of the calculation, is chosen to be (i) exactly solvable on a classical computer and (ii) practical to prepare and measure on a quantum device. The cost of implementing REM is solely attributed to the preparation of the reference state on a quantum device and the determination of its exact/noiseless energy using a classical computer. Provided that the reference state is also the initial state, there is no need for additional measurements of the reference state's energy on a quantum device.

The first work on REM demonstrated the use of a single-reference Hartree–Fock (HF) state to achieve significant error mitigation gains.[28] The HF state, described as an "uncorrelated" single determinant, can be easily prepared on a quantum computer using only Pauli-X gates. The circuits for HF state preparation maintain a constant complexity and are Clifford circuits, which can be efficiently simulated classically, as stated by the Gottesman–Knill theorem.[49] The HF state serves as the starting point for many wavefunction theories and ensures sufficient overlap with the target ground state in most molecules.[15,16,50] The effectiveness of using an HF reference for REM has subsequently been repeatedly demonstrated, *e.g.*, in ref. 28, 48 and 51. In contrast, random references generated from Clifford groups are almost guaranteed to be ineffective. The REM method combined with single-reference states such as HF nearly establishes a lower bound on QEM costs for quantum chemistry applications, as it incurs only the classical computational cost of a trivial state.

Although REM has proven effective in weakly correlated systems, its utility is more limited in the presence of strong electron correlation, such as in bond-stretching regions.[28] This limitation arises because REM assumes that the chosen reference state—typically a single Slater determinant (*e.g.*, Hartree–Fock)—is a reasonable approximation of the target ground state. However, in systems with strong correlation, the exact wavefunction often takes the form of a multireference (MR) state, *i.e.*, a linear combination of multiple Slater determinants (SDs) with similar weights. In such cases, a single determinant no longer provides sufficient overlap with the true ground state, and using it as a reference leads to inaccurate error mitigation. Consequently, REM becomes unreliable for these problems, motivating the need for an extended framework that incorporates multiconfigurational states with better overlap to the correlated target wavefunction.

In this work, we address this limitation by introducing multireference-state error mitigation (MREM), an extension of REM that systematically incorporates MR states into the error mitigation protocol. MREM uses approximate MR wavefunctions generated by inexpensive conventional methods and prepares them on quantum hardware using physically motivated, symmetry-preserving quantum circuits. In particular, we employ Givens rotations to construct multireference states with controlled expressivity and efficient hardware implementation.

While Givens rotations are central to our implementation, several other techniques exist for MR state preparation. These include low-depth adaptive ansätze,[52,53] adiabatic state preparation,[54,55] non-orthogonal subspace methods,[56–58] matrix product state preparation[59–62] and direct compilation techniques for arbitrary quantum states.[63,64] While each method offers its own advantages—in particular, compact circuits or systematic entanglement control—they frequently sacrifice exact symmetry preservation, entail intricate gate layouts, or demand significant ancillary resources. In contrast, Givens rotations offer a structured and physically interpretable approach to building linear combinations of SDs from a single reference configuration. They preserve key symmetries such as particle number and spin projection, and are known to be universal for quantum chemistry state preparation tasks.[65] These features, along with widespread prior use in constructing symmetry-adapted ansätze,[65–69] make Givens-based circuits a compelling and efficient choice for implementing MREM (see Section II D).

To avoid confusion, we want to note that the "multi-reference"-states used in MREM are not necessarily obtained through conventional quantum chemistry multireference methods. Rather, they refer to truncated multi-determinant wavefunctions,*i.e.*, a linear combination of SDs, derived from various classical methods including both single- and multi-reference approaches, as detailed below.

The rest of this paper is organized as follows. In Section II, we provide the basic concepts of VQE, an overview of the original REM, the basics of Givens rotations, and the methodology for realizing MREM using Givens rotations. Section III outlines computational details. In Section IV, we demonstrate the performance improvements of MREM compared to single-reference REM for the molecular systems H_2O, N_2, and F_2. Finally, Section V offers our conclusions and perspectives on the future directions of the MREM method.

II. Theory

A. The variational quantum eigensolver

While REM and our extension MREM do not rely on any specific variational algorithm, we have chosen to demonstrate the approach in the framework of VQE—perhaps the most well-known variational quantum algorithm—for familiarity. The electronic Hamiltonian $\hat{H}$ of a molecular system can be expressed in second quantization as

$$\hat{H} = \sum_{pq} h_p^q \hat{a}_p^\dagger \hat{a}_q + \frac{1}{2} \sum_{pqrs} g_{pq}^{rs} \hat{a}_p^\dagger \hat{a}_q^\dagger \hat{a}_s \hat{a}_r, \tag{1}$$

where ${h_p}^q$ and ${g_{pq}}^{rs}$ represent the one- and two-electron integrals, and $\hat{a}_p^{(\dagger)}$ represent the fermionic annihilation (creation) operators in spin-orbital p. In quantum computing, a fermion-to-qubit mapping such as the Jordan–Wigner (JW)[70] or Bravyi–Kitaev[71] transformation is required to convert the fermionic Hamiltonian, eqn (1), into a qubit Hamiltonian, expressed as a sum of N-qubit Pauli operators $\hat{P}_\alpha$:

$$\hat{H} = \sum_\alpha h_\alpha \hat{P}_\alpha, \tag{2}$$

with coefficients h_α. The VQE algorithm aims to find $E(\boldsymbol{\theta})$, an approximation to the ground state energy E_0 dependent on circuit parameters $\boldsymbol{\theta}$ such that

$$E_0 \leq E(\boldsymbol{\theta}) = \min_{\boldsymbol{\theta}} \langle \psi(\boldsymbol{\theta}) | \hat{H} | \psi(\boldsymbol{\theta}) \rangle. \tag{3}$$

We employ an ansatz, a parameterized quantum circuit $\hat{U}(\boldsymbol{\theta})$ to prepare a trial quantum state $|\psi(\boldsymbol{\theta})\rangle = \hat{U}(\boldsymbol{\theta})|\psi_0\rangle$, and calculate the energy expectation value from many measurements. The number of measurements (shots) for energy estimation using the molecular Hamiltonian scales as $\mathcal{O}(N^4/\epsilon^2)$, where ϵ is the desired precision and N is the number of qubits. The ansatz structure enables a quantum computer to explore a wide range of quantum states within a constrained expressible subspace, with optimization of its parameters guiding the search within this space. The state $|\psi_0\rangle = \hat{U}_{\text{init}}|0\rangle$ is an initial state that, optimally, has a large overlap with the ground state.

B. Reference-state error mitigation

Noise in the quantum system disrupts state preparation and measurements in quantum algorithms, like the VQE, limiting the ansatz's accessible space. Consequently, the energy estimate from the noisy VQE will be significantly higher than the true ground state energy. REM can effectively mitigate VQE energy errors by capturing the energy error caused by noise in a well-chosen reference state.

The procedure of REM, as applied to VQE, proceeds as follows: first, a reference state $|\psi_{\text{ref}}\rangle$ is selected, and its exact or noiseless energy $E_{\text{exact}}(\boldsymbol{\theta}_{\text{ref}})$ is determined using a classical computer. Next, this reference state is prepared on a quantum computer, and the corresponding noisy energy $E_{\text{VQE}}(\boldsymbol{\theta}_{\text{ref}})$ is measured. The effect of noise on the reference state is then quantified by the difference $\Delta E_{\text{REM}} = E_{\text{VQE}}(\boldsymbol{\theta}_{\text{ref}}) - E_{\text{exact}}(\boldsymbol{\theta}_{\text{ref}})$. Subsequently, the VQE algorithm is executed using the same circuit structure as used for preparing the reference state, yielding a noisy energy estimate $E_{\text{VQE}}(\boldsymbol{\theta}_{\text{min,VQE}})$ corresponding to the optimized parameters. Finally, the REM correction is applied to obtain an error-mitigated energy:

$$E_{\text{REM}}(\boldsymbol{\theta}_{\text{min,VQE}}) = E_{\text{VQE}}(\boldsymbol{\theta}_{\text{min,VQE}}) - \Delta E_{\text{REM}}. \tag{4}$$

A good first choice of $|\psi_{\text{ref}}\rangle$ is the single-reference HF state:

$$|\psi_{\text{HF}}\rangle = \hat{a}_{p1}^\dagger \hat{a}_{p2}^\dagger \cdots \hat{a}_{pne}^\dagger |0\rangle^{\otimes 2m} = |0\cdots 01\cdots 11\rangle, \tag{5}$$

where n_e denotes the number of electrons, and $2m$ is the total number of spin-orbitals. In this work, we chose an interleaved spin ordering of electrons for a Slater determinant. For instance, a generic singlet ($S_z = 0$) HF state is represented as $|0\cdots 01\cdots 11\rangle$, *i.e.*, $|\cdots n_{n\alpha+1}^\alpha n_{n\beta}^\beta \cdots n_1^\beta n_1^\alpha\rangle$, where the rightmost qubit refers to the first qubit, and $n_i^{\alpha,\beta} \in \{0,1\}$ represent the occupation number of spin-orbitals with electron spins α or β. Here, $n_\alpha = n_\beta = n_e/2$ indicate the number of each spin for the $S_z = 0$ state. In the JW mapping, each qubit corresponds to a spin-orbital of the molecular system, where the $|0\rangle$ and $|1\rangle$ states locally encode the occupation of each spin-orbital.

C. Multireference-state error mitigation

As outlined previously, the REM framework is general and can accommodate any reference state that is both practical to prepare on a quantum device and exactly solvable on a classical computer. The multireference-state error mitigation (MREM) strategy presented here constitutes a specific instantiation of REM, in which the reference state is a multiconfigurational wavefunction. The primary distinction between MREM and earlier single-reference REM implementations lies in Steps 1 and 2 of the general procedure (see Section II B). These steps involve the selection and preparation of a multireference (MR) state—a superposition of multiple Slater determinants—to better approximate the correlated electronic structure of the system:

$$|\psi_{\text{MR}}\rangle = \sum_j c_j |n_N \cdots n_2 n_1\rangle. \tag{6}$$

As illustrated in Fig. 1(a), the steps of MREM are:

(1) Select a suitable (possibly truncated) MR state guided by conventional quantum chemistry theories and determine its exact/noiseless energy with affordable cost on a classical computer.

(2) Prepare the MR state on quantum hardware (here using Givens rotations, see Section IID) and measure its noisy energy $E_{\text{VQE}}(\boldsymbol{\theta}_{\text{ref}})$ for the complete circuit (see Fig. 1(c)). The noise-induced deviation of the MR state is quantified as

$$\Delta E_{\text{MREM}} = E_{\text{VQE}}(\boldsymbol{\theta}_{\text{ref}}) - E_{\text{exact}}(\boldsymbol{\theta}_{\text{ref}}).$$

(3) Run the VQE optimization with the identical circuit used in the previous step to extract the noisy ground-state energy $E_{\text{VQE}}(\boldsymbol{\theta}_{\text{min,VQE}})$.

(4) Subtract the previously determined energy offset ΔE_{MREM} to yield the error-mitigated result:

$$E_{\text{MREM}}(\boldsymbol{\theta}_{\text{min,VQE}}) = E_{\text{VQE}}(\boldsymbol{\theta}_{\text{min,VQE}}) - \Delta E_{\text{MREM}}.$$

Importantly, in steps 2 and 3, we maintain consistency of circuit structure by employing the identical full circuit—comprising both state preparation and ansatz—across all noisy measurements, whether of the reference state or of the VQE-optimized ground state. This ensures that any observed discrepancies in measurement outcomes stem solely from

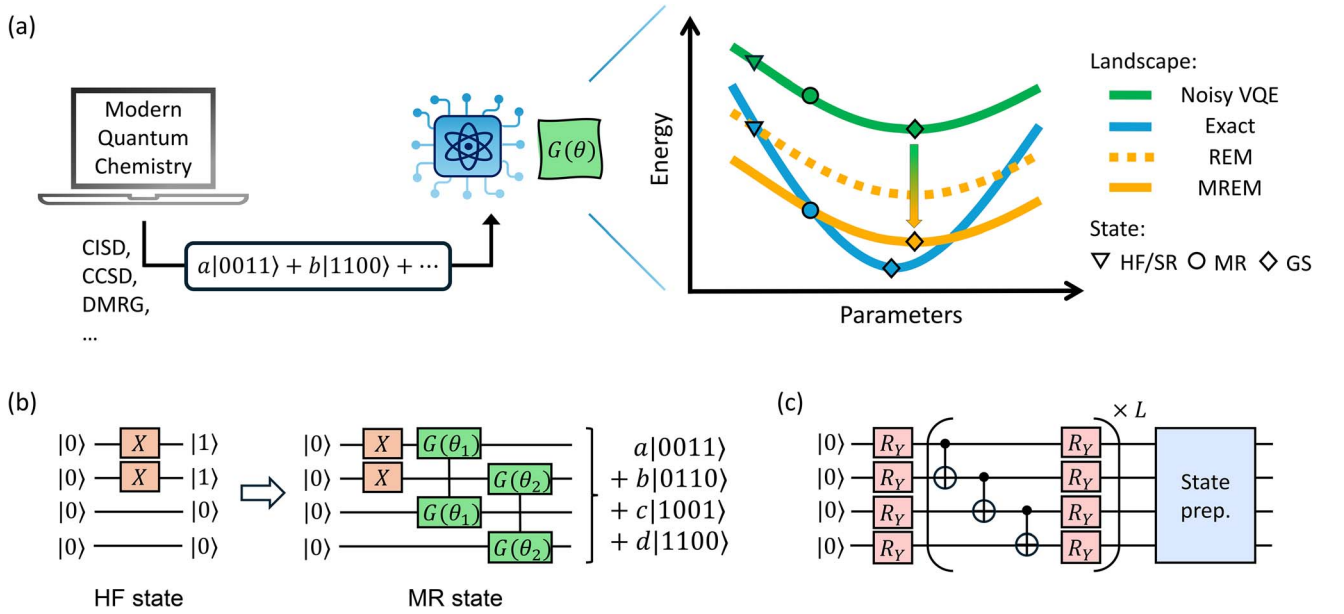

Fig. 1 Givens-based MREM method description. (a) The workflow begins with conventional quantum chemistry methods (*e.g.*, CISD, CCSD, DMRG) evaluating MR states, which are subsequently prepared on quantum hardware through Givens rotations. This MREM approach provides enhanced error mitigation capabilities compared to the single-reference REM methods, as illustrated in the energy landscape diagram where the MREM solutions (orange solid line) better approximate the exact solution (blue line) compared to the single-reference approaches (orange dashed line). (b) A MR state preparation circuit: parameterized Givens rotations generate excited configurations from an HF state. (c) Schematic of the complete quantum circuit used in this work. A hardware-efficient ansatz, comprising R_Y single-qubit rotations and a linearly entangling layer of CNOT gates, is placed before the state preparation circuit. By placing the ansatz in front and initializing all parameters to zero, the HEA acts as the identity on an initial $|0\rangle^{\otimes n}$ state in the noiseless case. However, under noisy execution, it introduces gate noise, thereby ensuring that both the reference and VQE-optimized energy measurements are affected by identical circuit-level noise, enabling consistent error mitigation.

differences in the states themselves, rather than from variations in the noise characteristics of different circuit implementations.

Our Givens-based MREM implementation is designed to flexibly incorporate MR states derived from a range of conventional quantum chemistry methods that capture electron correlation. In this work, we demonstrate this flexibility using MR states obtained from post-Hartree–Fock single-reference methods such as configuration interaction with singles and doubles (CISD)[72] and coupled cluster with singles and doubles (CCSD),[73] as well as multireference methods like the density matrix renormalization group (DMRG).[74]

While this versatility is a strength of the approach, it also introduces practical challenges in implementation. A key concern is the efficient preparation of the chosen MR states on quantum hardware without incurring excessive circuit complexity. If state preparation becomes too costly in terms of gate depth or non-Clifford resources, the additional noise can negate the benefits of improved expressivity. To address this trade-off, we employ truncated wavefunctions that retain only a small number of significant configurations—2–3 SDs in this work—aligning closely with the principles of selected configuration interaction[75,76] or full configuration interaction quantum Monte Carlo.[77–80] This simplification strikes a practical balance between error mitigation performance and the cost of additional circuit depth and noise.

D. Givens rotations

Givens rotations provide a computationally efficient framework for implementing the transformations required in the preparation of MR states within quantum circuits. In our approach, MR states are constructed by applying a sequence of Givens rotations to a single-reference determinant, systematically introducing electronic excitations to generate coherent superpositions of multiple Slater determinants.

Mathematically, a Givens rotation operates through a unitary transformation matrix that acts on two selected elements while leaving others unchanged. The fundamental block matrix takes the form

$$U(\theta) = \begin{pmatrix} \cos(\theta/2) & -\sin(\theta/2) \\ \sin(\theta/2) & \cos(\theta/2) \end{pmatrix}. \quad (7)$$

These rotations serve as fundamental operators that enable precise control over configuration state mixing. Importantly, they can preserve critical physical symmetries, notably the particle number conservation and the z-projection of the system's total spin, m_s. The particle number conservation is manifested through the commutation relation $[\hat{G}, \hat{N}] = 0$, where $\hat{N}$ is the particle-number operator. Conservation of m_s is achieved by restricting rotations to operations between same-spin orbitals.

In the context of quantum circuit implementation, consider the extension of eqn (7) to a $d = 2$ Hilbert subspace:

$$G(\theta) = \begin{pmatrix} 1 & 0 & 0 & 0 \\ 0 & \cos(\theta/2) & -\sin(\theta/2) & 0 \\ 0 & \sin(\theta/2) & \cos(\theta/2) & 0 \\ 0 & 0 & 0 & 1 \end{pmatrix} :=$$ 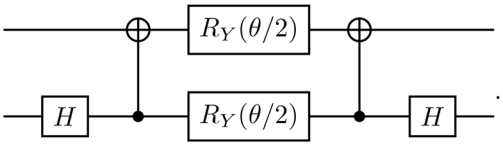

(8)

The rotation $G(\theta)$ can mix the $|01\rangle$ and $|10\rangle$ basis states while leaving the $|00\rangle$ and $|11\rangle$ states unchanged. Under the JW mapping, this operation corresponds to a single-electron excitation among spin-orbitals (without considering its parity).

Beyond single excitations, the Givens framework can be extended to describe higher-order excitations. In particular, the four-qubit "double-excitation" Givens rotation $G^{(2)}(\theta)$, which rotates the $|0011\rangle$ and $|1100\rangle$ states as follows:

$$\begin{aligned} G^{(2)}(\theta)|0011\rangle &= \cos(\theta/2)|0011\rangle + \sin(\theta/2)|1100\rangle, \\ G^{(2)}(\theta)|1100\rangle &= \cos(\theta/2)|1100\rangle - \sin(\theta/2)|0011\rangle. \end{aligned} \tag{9}$$

The decomposition of $G^{(2)}(\theta)$ into one- and two-qubit gates is shown in the ESI.[81]

In addition, controlled Givens rotations are introduced to guarantee universality in our circuit design. Formally, a controlled single-excitation rotation, $CG(\theta)$, acts on a three-qubit subspace by applying a Givens rotation to two target qubits conditioned on the control qubit being in the $|1\rangle$ state:

$$\begin{aligned} CG(\theta)|1ab\rangle &= |1\rangle \otimes G(\theta)|ab\rangle, \\ CG(\theta)|0ab\rangle &= |0\rangle \otimes |ab\rangle, \end{aligned} \tag{10}$$

where $|ab\rangle$ denotes the state of the two target qubits. Controlled Givens rotations enable the selective excitation of a specific configuration within a superposition. As a result, individual components of a multireference state can be independently addressed and coherently manipulated.

E. Givens-based multireference state preparation

In the JW mapping, we consider the state $|0011\rangle \equiv$  as a single-reference state with two electrons and four spin-orbitals. Here, ● and ○ represent the α and β electron spins, respectively. This state can, for example, represent the HF state of the H_2 molecule near the equilibrium bond length using a minimal basis set.

Our approach prepares the multireference state by generating excited configurations from the single-reference state. This is achieved by rotating the diagonal-pair two-qubit $|01\rangle$ and $|10\rangle$ subspaces in the Fock space using Givens rotations. As shown in Fig. 1(b), the first Givens rotation $G(\theta_1)$ and the second Givens rotation $G(\theta_2)$ rotate the subspaces of qubits 1 and 3, and qubits 2 and 4, respectively. These rotations are applied to spin-orbitals with the same spin, thereby preserving m_s of the molecular system. The four SDs shown in Fig. 1(b) account for all possible spin-conserving configurations in our case:

$$a$$  $+ b$  $+ c$  $+ d$  $,$ (11)

where a, b, c, d are the coefficients of the respective SD.

Considering a more complicated example, the ground state of stretched H_2O (4e, 4o) (with four active electrons and orbitals), when truncated to the leading three configurations, is typically represented as $a|00001111\rangle + b|00110011\rangle + c|11001100\rangle$ (assuming HF molecular orbitals) in the JW mapping. This state can be prepared through the sequential application of generalized Givens rotations: $CG^{(2)}_{3;8,7,2,1}(\theta_2)\, G^{(2)}_{6,5,4,3}(\theta_1)|00001111\rangle$. Here, the first subscript in the $CG^{(2)}$ gate indicates the control qubit, while subsequent subscripts denote the target qubits. Both $G^{(2)}$ and $CG^{(2)}$ gates exclusively excite the HF determinant $|00001111\rangle$.

To reduce computational complexity, we adopt the qubit tapering approach that exploits inherent Hamiltonian symmetries, specifically $\mathbb{Z}_2$ Pauli symmetries.[82] This technique maps qubit operators into the optimal symmetry eigensectors, effectively eliminating redundant degrees of freedom and reducing the total qubit count required for the quantum simulation. For our H_2O (4e, 4o) example, qubit tapering reduces the reference state to a more compact form: $a|00001\rangle + b|00110\rangle + c|11001\rangle$. This tapered form is derived by examining the qubits removed by tapering and mapping the corresponding configurations from the full Hilbert space onto the reduced subspace.

However, in doing so, the transformation disrupts the direct correspondence between spin-orbital occupations and qubits, which means Givens rotations alone are no longer sufficient to construct general MR states. To address this, we introduce controlled-X gates, which enables the preparation of specific configurations in the reduced qubit space by conditionally modifying bitstring patterns. This provides a mechanism for realizing SDs that cannot be directly generated through Givens rotations alone due to the altered qubit mapping.

For our H_2O (4e,4o) example, the final gate sequence implementing the tapered MR state employs a subset of the general gate set {CG, G, CX}, and consists of the following operations:

$$CX_{4,1}CX_{4,5}G_{4,1}(\theta_2)CX_{2,3}G_{2,1}(\theta_1)|00001\rangle, \tag{12}$$

where the subscripts in $CX_{i,j}$ denote that i is the control qubit and j is the target qubit. This circuit is manually constructed to reproduce the tapered MR state, with CX gates ensuring correct excitation structure in the reduced qubit space.

The rotation parameters θ_1 and θ_2 are determined through the solution of the following system of equations:

$$\begin{cases} a = \cos(\theta_1/2)\cos(\theta_2/2), \\ b = \sin(\theta_1/2), \\ c = \cos(\theta_1/2)\sin(\theta_2/2), \end{cases} \quad (13)$$

where a, b, and c again directly correspond to the coefficients of the target MR states.

III. Computational details

A. Benchmark systems and reference states

We evaluate the performance improvement of MREM over single-reference REM in treating electron correlation by conducting noisy VQE simulations on three representative small molecular systems: H_2O, N_2, and F_2. While the ground states of N_2, H_2O and F_2 are reasonably well-described by single-reference methods at equilibrium geometry, bond dissociation processes demand methods capable of capturing strong correlation effects. These systems form a small, targeted subset for probing strong correlation in small molecules, particularly in bond-breaking regimes, thereby serving as useful test cases for evaluating quantum error mitigation strategies.

Second-quantized Hamiltonians with restricted HF orbitals were computed using `PySCF`,[83] with correlation-consistent basis sets: cc-pVDZ for H_2O and F_2, and cc-pVTZ for N_2. Active space electronic Hamiltonians were extracted *via* `ActiveSpaceTransformer` in `Qiskit`,[84] with active spaces of H_2O (4e, 4o), N_2 (6e, 6o), and F_2 (10e, 6o). All fermionic Hamiltonians were mapped to qubits using the JW mapping. Qubit tapering reduced the number of qubits as follows: H_2O (8 → 5), N_2 (12 → 8), and F_2 (12 → 8). Exact diagonalization of the resulting qubit Hamiltonians was conducted using the `NumPyMinimumEigensolver` algorithm.

The target MR states were obtained through conventional quantum chemistry methods including CISD, CCSD (using `PySCF`), and DMRG (using `block2`[85]). The resulting wavefunctions were converted into state vectors using the `import_state` function in `PennyLane`,[86] from which the relevant Slater determinants and their coefficients were extracted.[87]

Approximate MR states were constructed by selecting 2–3 dominant Slater determinants based on their weight in the full wavefunction. For H_2O, we used CCSD with a 6-31G basis set; for F_2, CISD with STO-6G; and for N_2, DMRG with cc-pVTZ. We note that the basis set used to generate the MR state does not need to match that of the target Hamiltonian; smaller basis sets can still provide sufficiently accurate coefficients for the limited number of retained determinants, significantly reducing classical computational cost.

For the wavefunction ansatz, we employed a hardware-efficient ansatz (HEA), specifically the R_Y-linear ansatz $\hat{U}_{R_Y}(\boldsymbol{\theta})$, with 5 layers for H_2O, F_2, and 20 layers for N_2.[50] This ansatz is well suited to near-term quantum hardware due to its shallow depth, compatibility with native gate sets, and adaptability to device-specific connectivity constraints. However, it is known to suffer from trainability and optimization challenges,[88] particularly in systems involving more than 20 qubits.

Table 1 The number of qubits (#qbs), the number of repeated layers, L, in the R_Y-linear ansätze, the theoretical sources for MR states, and the number of prepared SDs for each simulated system

System	#qbs	L	MR source	# SDs
H_2O (4e, 4o; cc-pVDZ)	5	5	CCSD/6-31G	3
F_2 (10e, 6o; cc-pVDZ)	8	5	CISD/STO-6G	2
N_2 (6e, 6o; cc-pVTZ)	8	20	DMRG/cc-pVTZ	3

In the context of MREM, the interplay between the ansatz and state preparation circuits also requires careful consideration, especially regarding their ordering and initialization behavior on quantum hardware. Concerning the initial state preparation, it is important to point out that $\hat{U}_{R_Y}$ only acts trivially as the identity on the all-0 state, $\hat{U}_{R_Y}(0)|0\rangle = |0\rangle$ for $\boldsymbol{\theta} = 0$. Finding parameters for which $\hat{U}_{R_Y}(\boldsymbol{\theta})$ acts as the identity on a general initial state is not trivial. Thus, we place the R_Y-linear ansätze before the state preparation circuit, *i.e.*, $\hat{U}_{\text{init}}\hat{U}_{R_Y}|0\rangle$ instead of $\hat{U}_{R_Y}\hat{U}_{\text{init}}|0\rangle$, as shown in Fig. 1(c).

Table 1 summarizes key variables for each system, including the number of qubits after tapering, ansatz depth, reference wavefunction source, and the number of Slater determinants used.

B. Quantum circuit implementation and noise modeling

Quantum circuits and the VQE algorithm were implemented using the `Estimator` module of `Qiskit Aer 0.13.1`. For all `Estimator` simulations, each energy evaluation was estimated using 1×10^7 sampling shots. To accelerate simulations, we enabled the `approximation` option of the `Estimator`, which approximates the sampling distribution of measurement outcomes as a normal distribution. This `approximation` method significantly improves efficiency by avoiding explicit sampling, while still incorporating statistical noise. However, this method does not model readout errors, and therefore our results primarily reflect the effects of gate noise.

Noise simulations were performed using the `FakeSydneyV2` backend noise model, which incorporates depolarization and thermal relaxation errors on all single- and two-qubit gates. Device-specific noise parameters, including gate errors, durations, readout errors, and decoherence times, were derived from real IBM device calibration data.[89]

For variational optimization, we used a gradient-free classical optimizer based on the implicit filtering (ImFil) algorithm, as implemented in the `scikit-quant` package.[90] This optimizer is well suited for noisy, high-dimensional landscapes with many local minima.

C. Enforcing spin symmetry

HEA, while favored for their low circuit depth and hardware compatibility, do not inherently preserve physical symmetries. This lack of symmetry adaptation can result in qualitatively incorrect variational states, manifesting as nondifferentiable

cusps in potential energy surfaces (PES) and significant spin contamination.[91] Such issues are particularly pronounced in systems like H_2O and N_2, where an accurate description of the singlet ground state is essential. Quantum noise further exacerbates symmetry breaking, as gate errors and decoherence can push the variational state out of the desired symmetry sector.

To address these symmetry-breaking effects, we introduce a spin penalty term into the qubit Hamiltonian: $\hat{H}' = \hat{H} + \lambda \cdot \hat{\boldsymbol{S}}^2$, where $\hat{\boldsymbol{S}}^2$ is the total spin angular momentum operator and $\lambda > 0$ is a tunable penalty coefficient. Since our goal is to recover the singlet ground state ($S = 0$), this penalty lowers the energy of spin-pure singlet states relative to spin-contaminated alternatives. Importantly, this linear penalty form exploits the fact that the eigenvalues of $\hat{\boldsymbol{S}}^2$ are non-negative and minimized for singlets. Unlike the standard squared deviation formulation, $\lambda \cdot (\mathbf{S}^2 - S(S+1))^2$,[16] this linear variant avoids introducing a large number of additional Pauli terms, thereby reducing measurement overhead in noisy simulations.

In our simulations, we set $\lambda = 0.1$ for H_2O and $\lambda = 0.5$ for N_2, based on empirical tuning. These values were sufficient to suppress spin contamination and stabilize VQE convergence without significantly distorting the underlying energy landscape. For F_2, where the HEA did not lead to appreciable symmetry breaking, no penalty term was applied.

IV. Results and discussion

In this section, we evaluate the performance of MREM by computing potential energy surfaces for our collection of molecules: H_2O, N_2, and F_2. Fig. 2 shows comparisons between MREM and single-reference REM. In this figure, VQE results using an HF initial state is labeled as "VQE-HF", while the corresponding REM-corrected curve is denoted by "REM-HF". Similarly, the VQE data calculated using a linear combination of n SDs (Table 1) as initial state (and reference) is labeled "VQE-nSDs", while its corresponding MREM-correction is denoted by "MREM-nSDs".

Note also that in these tests, we compare to a computational accuracy. The latter threshold is defined as an error of 1.6×10^{-3} hartree (1 kcal mol^{-1}) with respect to the exact result obtained in the complete absence of noise, using the same level of theory. We make this point because a given level of theory need not be exact with respect to reality. In other words, a calculation with computational accuracy need not have the chemical accuracy needed for realistic chemical predictions, a distinction suggested in ref. 28.

For H_2O the MR state is constructed using three dominant Slater determinants *via* two-qubit Givens rotations (eq. (8)), enabling efficient generation of single excitations. Due to the additional circuit complexity, the VQE-3SDs results exhibit higher energy compared to VQE-HF, as depicted in Fig. 2(a). However, after applying the REM correction, MREM-3SDs yields a substantial reduction in error and recovers a more accurate potential energy surface. This highlights the importance of combining MR states with error mitigation: although MR states alone may not improve noisy VQE outcomes, they serve as a more expressive and physically grounded reference for the mitigation step. The gate-efficient MR construction thus enables MREM to extract meaningful physical information in noisy conditions, while keeping circuit overhead moderate.

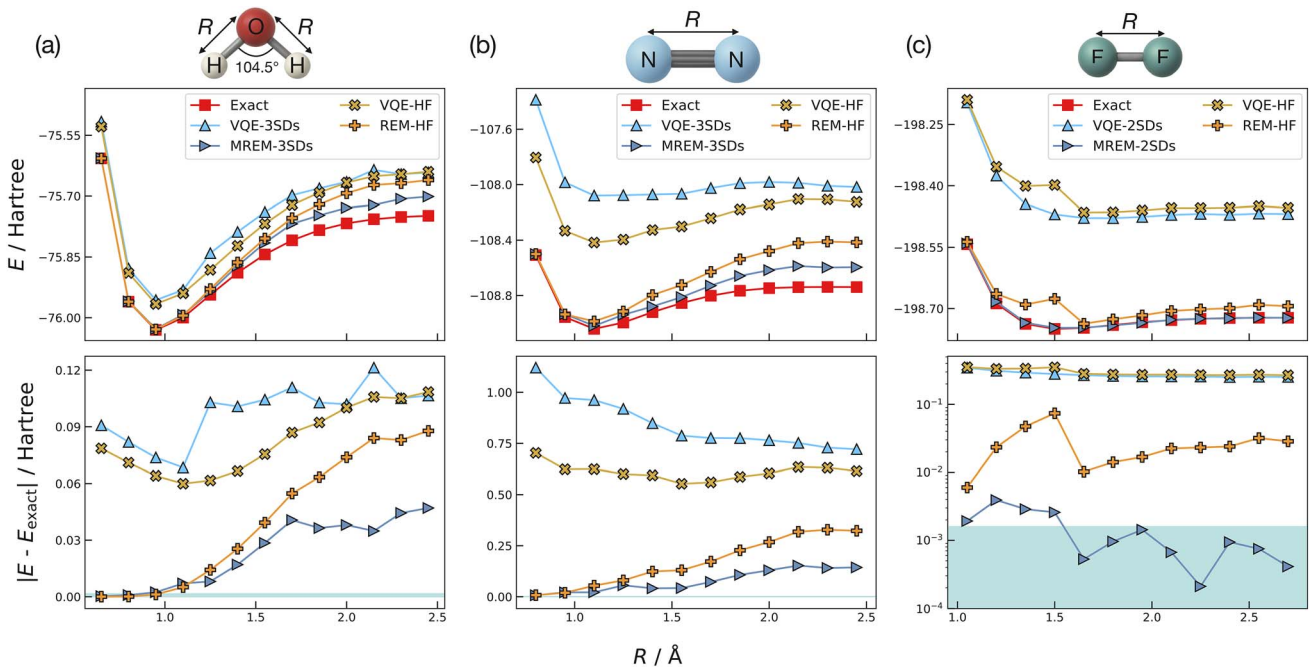

Fig. 2 Comparisons of MREM and single-reference REM for PESs. PESs (top) and absolute errors (bottom) are computed for (a) H_2O (4e, 4o; cc-pVDZ) symmetric stretching, (b) N_2 (6e, 6o; cc-pVTZ), and (c) F_2 (10e, 6o; cc-pVDZ) bond dissociation. The cyan-shaded areas represent the computational accuracy below 1.6×10^{-3} hartree (1 kcal mol^{-1}).

The N_2 molecule (Fig. 2(b)) presents a greater challenge due to its strong multireference character. Capturing the relevant correlation requires MR states with double excitations, implemented using four-qubit Givens rotations ($G^{(2)}$). However, the decomposition of $G^{(2)}$ is not gate-efficient (see the ESI[81]), resulting in substantial circuit depth and elevated noise. Consequently, the unmitigated VQE-3SDs performs worse than VQE-HF in both energy accuracy and the overall PES profile. Nonetheless, the error-mitigated MREM-3SDs recovers much of the expected physical behavior in the bond-stretching region. The improved PES shape and consistently reduced errors demonstrate that when facing a balance between expressivity and circuit complexity, using MR states can provide clear advantages when combined with error mitigation.

The F_2 molecule (Fig. 2(c)) is a prototypical example where a compact MR state with two selected SDs suffices to capture the essential near-degeneracy between bonding σ and antibonding σ^* orbitals during bond-stretching region. This leads to near-computational accuracy in MREM-2SDs, with errors reduced by approximately two orders of magnitude compared to the noisy VQE results and by one order of magnitude compared to the REM-HF results. Despite the additional noise in MREM-2SDs circuits, the MR state provides a better initialization that improves convergence during VQE optimization, particularly in regions where $R \leq 1.5$ Å, where noisy VQE often fails due to local minima.

We additionally include the initial energies of both the exact and noisy MR states in the ESI.[81] Due to hardware noise, noisy VQE only provides lower energies than the noisy MR initial states in the H_2O bond-stretching region. In all other cases noisy MR provides lower energies. Importantly however, our MREM-corrected VQE results consistently surpass the exact MR initial energies.

V. Conclusion and outlook

In this work, we have developed a multireference error mitigation (MREM) framework for improving quantum simulations of strongly correlated molecular systems. Central to this approach is the preparation of multireference (MR) states that exhibit substantial overlap with the target ground state, constructed from conventional quantum chemistry methods such as configuration interaction, coupled cluster, or the density matrix renormalization group. We introduce an efficient and physically motivated scheme to prepare these states on quantum hardware using Givens rotations, and validate the resulting Givens-based MREM framework through noisy digital quantum simulations of H_2O, N_2, and F_2. Our results demonstrate two key advantages: (i) MR references enhance REM performance over single-determinant schemes, providing physically motivated energy error mitigation at low cost, and (ii) Givens-encoded MR states serve as robust initializations for VQE, reducing the risk of becoming trapped in local minima and accelerating convergence (see the ESI[81]). While increasing the number of reference states can introduce additional circuit noise, our results suggest that the improved mitigation performance outweighs this cost—particularly in shallow circuit regimes relevant to near-term hardware.

MREM is an error mitigation framework that can be integrated with a broad class of variational quantum algorithms beyond VQE, offering flexibility for near-term quantum chemistry applications. Within this framework, the primary scalability challenge arises from the circuit complexity required for MR state preparation, which represents the most essential and resource-intensive subroutine. To address this resource bottleneck, future work will focus on developing more compact circuit constructions that preserve essential physical symmetries while reducing gate overhead. Promising directions include combining MREM with spin-conserving methods,[66,80,92–103] explicitly correlated methods,[104–108] especially the transcorrelated approach,[19,48,109–116] tiled unitary product states[68,117] as well as the separable-pair approximation.[118,119]

Another promising avenue for enhancing MREM lies in exploring the expressivity differences between Clifford and near-Clifford ansatz states. For instance, an open question is whether Clifford circuit initialization, which restricts single-qubit rotation gates in the HEA to discrete multiples of $\pi/2$,[120] can enhance the performance of our Givens-based MR circuit in approximating the ground state.

We have also identified several broader opportunities for enhancing the MREM framework itself. Because MREM achieves noise reduction by exploiting the inherent classical simulatability of select MR circuits, one can imagine viewing such circuits as being classical post-processing operators, in accordance with the Schrödinger–Heisenberg VQE paradigm.[121] Such an approach could strategically offload circuit complexity to classical devices, leading to shallower quantum circuits that are more resilient to noise. We also plan to extend (M)REM to observables beyond the energy, such as dipole moments, in future work. Finally, given MREM's fixed circuit structure designed to prevent noisy gate variable effects, its integration with adaptive ansätze[52,122] using statistical tools merits investigation.

We want to underscore that MREM can be integrated with other quantum error mitigation (QEM) techniques. For instance, the original REM study demonstrated its compatibility with measurement error mitigation.[28] Moreover, by applying controlled noise amplification to both MR and VQE states and performing polynomial or exponential extrapolation,[26,35] one can correct for higher-order noise contributions that MREM alone does not directly address, thereby enhancing overall error-mitigation performance. In addition, MREM can be extended to a data-driven framework. For instance, the idea of using REM-derived training data has appeared in ref. 123, albeit without the chemical intuition that MREM brings, and it echoes the spirit of Clifford data regression.[42] By unifying the heterogeneous data sources (such as noise extrapolated data and reference enhancement data), one can promisingly harness the complementary strengths of diverse QEM techniques.[43]

One possible next step is to scale MREM to over 20 qubits on a real quantum device, thereby providing a empirical assessment of its practicality for larger realistic systems. A key practical consideration is the backend compilation pipeline: the rotation unitaries treated here as ideal, high-level primitives are not executed verbatim on hardware but are decomposed into the native gate set of each architecture. The resulting pattern of

gate commutation, gate cancellation or operation scheduling is highly sensitive to the transpiler's layout heuristics, optimization level and device topology.[124,125] Consequently, benchmarking MREM across platforms requires either fixing the compilation workflow or reporting it in full; otherwise, the post-transpilation noise profile may obscure—or even exaggerate—the intrinsic advantages conferred by the MR state. Furthermore, in cases where the target MR state requires excitations spanning multiple spin orbitals, the resulting long-range entanglement demands can further exacerbate the connectivity constraints of hardware with limited coupling maps.

Conflicts of interest

There are no conflicts to declare.

Data availability

The data and code for the study reported in this article can be found on the Zenodo repository: **https://doi.org/10.5281/zenodo.15827822**.[126] The version of the code and data employed for the analyses presented in this article is the archived release as of 7 July 2025.

In addition to the deposited repository, we provide extensive reference data—including computed values, tabulated results, and benchmark comparisons. See DOI: **https://doi.org/10.1039/d5dd00202h**.

Acknowledgements

Funded by the European Union. Views and opinions expressed are, however, those of the author(s) only and do not necessarily reflect those of the European Union or REA. Neither the European Union nor the granting authority can be held responsible for them. This work was funded by the EU Flagship on Quantum Technology HORIZON-CL4-2022-QUANTUM-01-SGA project 101113946 OpenSuperQPlus100. This research has been supported by funding from the Wallenberg Center for Quantum Technology (WACQT). WD acknowledges funding from the European Union's Horizon Europe research and innovation program under the Marie Skłodowska-Curie grant agreement No. 101062864 and the German Federal Ministry of Research, Technology and Space (BMFTR) under the research program Quantensysteme and funding measure Quantum Futur 3 for project No. 13N17229. This research relied on computational resources provided by the National Academic Infrastructure for Supercomputing in Sweden (NAISS) at C3SE and NSC, partially funded by the Swedish Research Council through grant agreement no. 2022-06725.

References

1 S. Boixo, S. V. Isakov, V. N. Smelyanskiy, R. Babbush, N. Ding, Z. Jiang, M. J. Bremner, J. M. Martinis and H. Neven, Characterizing quantum supremacy in near-term devices, *Nat. Phys.*, 2018, **14**, 595.
2 F. Arute, K. Arya, R. Babbush, D. Bacon, J. C. Bardin, R. Barends, R. Biswas, S. Boixo, F. G. Brandao, D. A. Buell, *et al.*, Quantum supremacy using a programmable superconducting processor, *Nature*, 2019, **574**, 505.
3 Y. Wu, W.-S. Bao, S. Cao, F. Chen, M.-C. Chen, X. Chen, T.-H. Chung, H. Deng, Y. Du, D. Fan, *et al.*, Strong quantum computational advantage using a superconducting quantum processor, *Phys. Rev. Lett.*, 2021, **127**, 180501.
4 R. P. Feynman, Simulating physics with computers, in *Feynman and computation*, CRC Press, 2018, pp. 133–153.
5 S. Lloyd, Universal quantum simulators, *Science*, 1996, **273**, 1073.
6 B. Fauseweh, Quantum many-body simulations on digital quantum computers: State-of-the-art and future challenges, *Nat. Commun.*, 2024, **15**, 2123.
7 A. Aspuru-Guzik, A. D. Dutoi, P. J. Love and M. Head-Gordon, Simulated quantum computation of molecular energies, *Science*, 2005, **309**, 1704.
8 B. P. Lanyon, J. D. Whitfield, G. G. Gillett, M. E. Goggin, M. P. Almeida, I. Kassal, J. D. Biamonte, M. Mohseni, B. J. Powell, M. Barbieri, *et al.*, Towards quantum chemistry on a quantum computer, *Nat. Chem.*, 2010, **2**, 106.
9 Y. Cao, J. Romero, J. P. Olson, M. Degroote, P. D. Johnson, M. Kieferová, I. D. Kivlichan, T. Menke, B. Peropadre, N. P. Sawaya, *et al.*, Quantum chemistry in the age of quantum computing, *Chem. Rev.*, 2019, **119**, 10856.
10 B. Bauer, S. Bravyi, M. Motta and G. K.-L. Chan, Quantum algorithms for quantum chemistry and quantum materials science, *Chem. Rev.*, 2020, **120**, 12685.
11 S. McArdle, S. Endo, A. Aspuru-Guzik, S. C. Benjamin and X. Yuan, Quantum computational chemistry, *Rev. Mod. Phys.*, 2020, **92**, 015003.
12 J. Preskill, Quantum computing in the nisq era and beyond, *Quantum*, 2018, **2**, 79.
13 D. Stilck França and R. Garcia-Patron, Limitations of optimization algorithms on noisy quantum devices, *Nat. Phys.*, 2021, **17**, 1221.
14 Y. Yan, Z. Du, J. Chen and X. Ma, Limitations of noisy quantum devices in computational and entangling power, *arXiv*, 2023, preprint, arXiv:2306.02836 [quant-ph], DOI: **10.48550/arXiv.2306.02836**.
15 A. Peruzzo, J. McClean, P. Shadbolt, M.-H. Yung, X.-Q. Zhou, P. J. Love, A. Aspuru-Guzik and J. L. O'brien, A variational eigenvalue solver on a photonic quantum processor, *Nat. Commun.*, 2014, **5**, 4213.
16 J. R. McClean, J. Romero, R. Babbush and A. Aspuru-Guzik, The theory of variational hybrid quantum-classical algorithms, *New J. Phys.*, 2016, **18**, 023023.
17 S. McArdle, T. Jones, S. Endo, Y. Li, S. C. Benjamin and X. Yuan, Variational ansatz-based quantum simulation of imaginary time evolution, *Npj Quantum Inf.*, 2019, **5**, 75.
18 X. Yuan, S. Endo, Q. Zhao, Y. Li and S. C. Benjamin, Theory of variational quantum simulation, *Quantum*, 2019, **3**, 191.
19 I. O. Sokolov, W. Dobrautz, H. Luo, A. Alavi and I. Tavernelli, Orders of magnitude increased accuracy for

quantum many-body problems on quantum computers via an exact transcorrelated method, *Phys. Rev. Res.*, 2023, **5**, 023174.
20 P. W. Shor, Fault-tolerant quantum computation, in *Proceedings of 37th conference on foundations of computer science*, IEEE, 1996, pp. 56–65.
21 A. G. Fowler, M. Mariantoni, J. M. Martinis and A. N. Cleland, Surface codes: Towards practical large-scale quantum computation, *Phys. Rev. A*, 2012, **86**, 032324.
22 D. A. Lidar and T. A. Brun, *Quantum error correction*, Cambridge university press, 2013.
23 N. P. Breuckmann and J. N. Eberhardt, Quantum low-density parity-check codes, *PRX Quantum*, 2021, **2**, 040101.
24 Z. Cai, R. Babbush, S. C. Benjamin, S. Endo, W. J. Huggins, Y. Li, J. R. McClean and T. E. O'Brien, Quantum error mitigation, *Rev. Mod. Phys.*, 2023, **95**, 045005.
25 S. Endo, Z. Cai, S. C. Benjamin and X. Yuan, Hybrid quantum-classical algorithms and quantum error mitigation, *J. Phys. Soc. Jpn.*, 2021, **90**, 032001.
26 K. Temme, S. Bravyi and J. M. Gambetta, Error mitigation for short-depth quantum circuits, *Phys. Rev. Lett.*, 2017, **119**, 180509.
27 S. Endo, S. C. Benjamin and Y. Li, Practical quantum error mitigation for near-future applications, *Phys. Rev. X*, 2018, **8**, 031027.
28 P. Lolur, M. Skogh, W. Dobrautz, C. Warren, J. Biznárová, A. Osman, G. Tancredi, G. Wendin, J. Bylander and M. Rahm, Reference-state error mitigation: A strategy for high accuracy quantum computation of chemistry, *J. Chem. Theory Comput.*, 2023, **19**, 783.
29 X. Bonet-Monroig, R. Sagastizabal, M. Singh and T. O'Brien, Low-cost error mitigation by symmetry verification, *Phys. Rev. A*, 2018, **98**, 062339.
30 W. J. Huggins, S. McArdle, T. E. O'Brien, J. Lee, N. C. Rubin, S. Boixo, K. B. Whaley, R. Babbush and J. R. McClean, Virtual distillation for quantum error mitigation, *Phys. Rev. X*, 2021, **11**, 041036.
31 H. Liao, D. S. Wang, I. Sitdikov, C. Salcedo, A. Seif and Z. K. Minev, Machine learning for practical quantum error mitigation, *Nat. Mach. Intell.*, 2024, **6**, 1478–1486.
32 S. Bravyi, S. Sheldon, A. Kandala, D. C. Mckay and J. M. Gambetta, Mitigating measurement errors in multiqubit experiments, *Phys. Rev. A*, 2021, **103**, 042605.
33 P. D. Nation, H. Kang, N. Sundaresan and J. M. Gambetta, Scalable mitigation of measurement errors on quantum computers, *PRX Quantum*, 2021, **2**, 040326.
34 J. R. McClean, M. E. Kimchi-Schwartz, J. Carter and W. A. De Jong, Hybrid quantum-classical hierarchy for mitigation of decoherence and determination of excited states, *Phys. Rev. A*, 2017, **95**, 042308.
35 Y. Li and S. C. Benjamin, Efficient variational quantum simulator incorporating active error minimization, *Phys. Rev. X*, 2017, **7**, 021050.
36 S. Endo, S. C. Benjamin and Y. Li, Practical quantum error mitigation for near-future applications, *Phys. Rev. X*, 2018, **8**, 031027.
37 B. Koczor, Exponential error suppression for near-term quantum devices, *Phys. Rev. X*, 2021, **11**, 031057.
38 A. Strikis, D. Qin, Y. Chen, S. C. Benjamin and Y. Li, Learning-based quantum error mitigation, *PRX Quantum*, 2021, **2**, 040330.
39 T. Takeshita, N. C. Rubin, Z. Jiang, E. Lee, R. Babbush and J. R. McClean, Increasing the representation accuracy of quantum simulations of chemistry without extra quantum resources, *Phys. Rev. X*, 2020, **10**, 011004.
40 M. Skogh, W. Dobrautz, P. Lolur, C. Warren, J. Biznárová, A. Osman, G. Tancredi, J. Bylander and M. Rahm, The electron density: a fidelity witness for quantum computation, *Chem. Sci.*, 2024, **15**, 2257–2265.
41 B. Yang, R. Raymond and S. Uno, Efficient quantum readout-error mitigation for sparse measurement outcomes of near-term quantum devices, *Phys. Rev. A*, 2022, **106**, 012423.
42 P. Czarnik, A. Arrasmith, P. J. Coles and L. Cincio, Error mitigation with Clifford quantum-circuit data, *Quantum*, 2021, **5**, 592.
43 D. Bultrini, M. H. Gordon, P. Czarnik, A. Arrasmith, M. Cerezo, P. J. Coles and L. Cincio, Unifying and benchmarking state-of-the-art quantum error mitigation techniques, *Quantum*, 2023, **7**, 1034.
44 R. Takagi, H. Tajima and M. Gu, Universal sampling lower bounds for quantum error mitigation, *Phys. Rev. Lett.*, 2023, **131**, 210602.
45 R. Takagi, S. Endo, S. Minagawa and M. Gu, Fundamental limits of quantum error mitigation, *Npj Quantum Inf.*, 2022, **8**, 114.
46 K. Tsubouchi, T. Sagawa and N. Yoshioka, Universal cost bound of quantum error mitigation based on quantum estimation theory, *Phys. Rev. Lett.*, 2023, **131**, 210601.
47 Y. Quek, D. Stilck França, S. Khatri, J. J. Meyer and J. Eisert, Exponentially tighter bounds on limitations of quantum error mitigation, *Nat. Phys.*, 2024, **20**, 1.
48 W. Dobrautz, I. O. Sokolov, K. Liao, P. L. Ríos, M. Rahm, A. Alavi and I. Tavernelli, Toward real chemical accuracy on current quantum hardware through the transcorrelated method, *J. Chem. Theory Comput.*, 2024, **20**, 4146–4160.
49 D. Gottesman, The heisenberg representation of quantum computers, *arXiv*, 1998, preprint, arXiv:quant-ph/9807006, DOI: 10.48550/arXiv.quant-ph/9807006.
50 A. Kandala, A. Mezzacapo, K. Temme, M. Takita, M. Brink, J. M. Chow and J. M. Gambetta, Hardware-efficient variational quantum eigensolver for small molecules and quantum magnets, *Nature*, 2017, **549**, 242.
51 J. A. de Gracia Triviño, M. G. Delcey and G. Wendin, Complete active space methods for nisq devices: The importance of canonical orbital optimization for accuracy and noise resilience, *J. Chem. Theory Comput.*, 2023, **19**, 2863.
52 H. R. Grimsley, S. E. Economou, E. Barnes and N. J. Mayhall, An adaptive variational algorithm for exact molecular simulations on a quantum computer, *Nat. Commun.*, 2019, **10**, 3007.

53 H. L. Tang, V. Shkolnikov, G. S. Barron, H. R. Grimsley, N. J. Mayhall, E. Barnes and S. E. Economou, qubit-adapt-vqe: An adaptive algorithm for constructing hardware-efficient ansätze on a quantum processor, *PRX Quantum*, 2021, **2**, 020310.
54 A. Aspuru-Guzik, A. D. Dutoi, P. J. Love and M. Head-Gordon, Simulated quantum computation of molecular energies, *Science*, 2005, **309**, 1704.
55 L. Veis and J. Pittner, Adiabatic state preparation study of methylene, *J. Chem. Phys.*, 2014, **140**, 214111.
56 W. J. Huggins, J. Lee, U. Baek, B. O'Gorman and K. B. Whaley, A non-orthogonal variational quantum eigensolver, *New J. Phys.*, 2020, **22**, 073009.
57 U. Baek, D. Hait, J. Shee, O. Leimkuhler, W. J. Huggins, T. F. Stetina, M. Head-Gordon and K. B. Whaley, Say no to optimization: A nonorthogonal quantum eigensolver, *PRX Quantum*, 2023, **4**, 030307.
58 N. H. Stair, R. Huang and F. A. Evangelista, A multireference quantum krylov algorithm for strongly correlated electrons, *J. Chem. Theory Comput.*, 2020, **16**, 2236.
59 D. W. Berry, Y. Tong, T. Khattar, A. White, T. I. Kim, G. H. Low, S. Boixo, Z. Ding, L. Lin, S. Lee, *et al.*, Rapid Initial-State Preparation for the Quantum Simulation of Strongly Correlated Molecules, *PRX Quantum*, 2025, **6**, 020327.
60 S.-J. Ran, Encoding of matrix product states into quantum circuits of one-and two-qubit gates, *Phys. Rev. A*, 2020, **101**, 032310.
61 C. Schön, E. Solano, F. Verstraete, J. I. Cirac and M. M. Wolf, Sequential generation of entangled multiqubit states, *Phys. Rev. Lett.*, 2005, **95**, 110503.
62 D. Malz, G. Styliaris, Z.-Y. Wei and J. I. Cirac, Preparation of matrix product states with log-depth quantum circuits, *Phys. Rev. Lett.*, 2024, **132**, 040404.
63 G. H. Low, V. Kliuchnikov and L. Schaeffer, Trading T gates for dirty qubits in state preparation and unitary synthesis, *Quantum*, 2024, **8**, 1375.
64 K. Gui, A. M. Dalzell, A. Achille, M. Suchara and F. T. Chong, Spacetime-efficient low-depth quantum state preparation with applications, *Quantum*, 2024, **8**, 1257.
65 J. M. Arrazola, O. Di Matteo, N. Quesada, S. Jahangiri, A. Delgado and N. Killoran, Universal quantum circuits for quantum chemistry, *Quantum*, 2022, **6**, 742.
66 G.-L. R. Anselmetti, D. Wierichs, C. Gogolin and R. M. Parrish, Local, expressive, quantum-number-preserving vqe ansätze for fermionic systems, *New J. Phys.*, 2021, **23**, 113010.
67 B. T. Gard, L. Zhu, G. S. Barron, N. J. Mayhall, S. E. Economou and E. Barnes, Efficient symmetry-preserving state preparation circuits for the variational quantum eigensolver algorithm, *Npj Quantum Inf.*, 2020, **6**, 10.
68 H. G. Burton, Accurate and gate-efficient quantum ansätze for electronic states without adaptive optimization, *Phys. Rev. Res.*, 2024, **6**, 023300.
69 C. H. Chee, D. Leykam, A. M. Mak and D. G. Angelakis, Shallow quantum circuits for efficient preparation of slater determinants and correlated states on a quantum computer, *Phys. Rev. A*, 2023, **108**, 022416.
70 P. Jordan and E. P. Wigner, *Über das paulische äquivalenzverbot*, Springer, 1993.
71 S. B. Bravyi and A. Y. Kitaev, Fermionic quantum computation, *Ann. Phys.*, 2002, **298**, 210.
72 R. J. Buenker and S. D. Peyerimhoff, Individualized configuration selection in ci calculations with subsequent energy extrapolation, *Theor. Chim. Acta*, 1974, **35**, 33.
73 J. Čížek, On the correlation problem in atomic and molecular systems. calculation of wavefunction components in ursell-type expansion using quantum-field theoretical methods, *J. Chem. Phys.*, 1966, **45**, 4256.
74 S. R. White, Density matrix formulation for quantum renormalization groups, *Phys. Rev. Lett.*, 1992, **69**, 2863.
75 B. Huron, J. P. Malrieu and P. Rancurel, Iterative perturbation calculations of ground and excited state energies from multiconfigurational zeroth-order wavefunctions, *J. Chem. Phys.*, 1973, **58**, 5745–5759.
76 Y. Garniron, A. Scemama, E. Giner, M. Caffarel and P.-F. Loos, Selected configuration interaction dressed by perturbation, *J. Chem. Phys.*, 2018, **149**, 064103.
77 G. H. Booth, A. J. W. Thom and A. Alavi, Fermion monte carlo without fixed nodes: A game of life, death, and annihilation in slater determinant space, *J. Chem. Phys.*, 2009, **131**, 054106.
78 K. Guther, R. J. Anderson, N. S. Blunt, N. A. Bogdanov, D. Cleland, N. Dattani, W. Dobrautz, K. Ghanem, P. Jeszenszki, N. Liebermann, G. L. Manni, A. Y. Lozovoi, H. Luo, D. Ma, F. Merz, C. Overy, M. Rampp, P. K. Samanta, L. R. Schwarz, J. J. Shepherd, S. D. Smart, E. Vitale, O. Weser, G. H. Booth and A. Alavi, Neci: N-electron configuration interaction with an emphasis on state-of-the-art stochastic methods, *J. Chem. Phys.*, 2020, **153**, 034107.
79 W. Dobrautz, O. Weser, N. A. Bogdanov, A. Alavi and G. Li Manni, Spin-pure stochastic-casscf via guga-fciqmc applied to iron–sulfur clusters, *J. Chem. Theory Comput.*, 2021, **17**, 5684–5703.
80 W. Dobrautz, S. D. Smart and A. Alavi, Efficient formulation of full configuration interaction quantum monte carlo in a spin eigenbasis via the graphical unitary group approach, *J. Chem. Phys.*, 2019, **151**, 094104.
81 SI available. See DOI: **https://doi.org/10.1039/d5dd00202h**.
82 S. Bravyi, J. M. Gambetta, A. Mezzacapo and K. Temme, Tapering off qubits to simulate fermionic hamiltonians, *arXiv*, 2017, preprint, arXiv:1701.08213, DOI: **10.48550/arXiv.1701.08213**.
83 Q. Sun, X. Zhang, S. Banerjee, P. Bao, M. Barbry, N. S. Blunt, N. A. Bogdanov, G. H. Booth, J. Chen, Z.-H. Cui, *et al.*, Recent developments in the pyscf program package, *J. Chem. Phys.*, 2020, **153**, 024109.
84 Qiskit Community, *Qiskit: An open-source framework for quantum computing*, 2017.

85 H. Zhai, H. R. Larsson, S. Lee, Z.-H. Cui, T. Zhu, C. Sun, L. Peng, R. Peng, K. Liao, J. Tölle, *et al.*, Block2: A comprehensive open source framework to develop and apply state-of-the-art dmrg algorithms in electronic structure and beyond, *J. Chem. Phys.*, 2023, **159**, 234801.
86 V. Bergholm, J. Izaac, M. Schuld, C. Gogolin, S. Ahmed, V. Ajith, M. S. Alam, G. Alonso-Linaje, B. AkashNarayanan, A. Asadi, *et al.*, Pennylane: Automatic differentiation of hybrid quantum-classical computations, *arXiv*, 2018, preprint, arXiv:1811.04968, DOI: **10.48550/arXiv.1811.04968**.
87 S. Fomichev, Initial state preparation for quantum chemistry, **https://pennylane.ai/qml/demos/tutorial_initial_state_preparation/**, 2023.
88 J. R. McClean, S. Boixo, V. N. Smelyanskiy, R. Babbush and H. Neven, Barren plateaus in quantum neural network training landscapes, *Nat. Commun.*, 2018, **9**, 4812.
89 C. J. Wood, Special session: Noise characterization and error mitigation in near-term quantum computers, in *2020 IEEE 38th International Conference on Computer Design (ICCD)*, IEEE, 2020, pp. 13–16.
90 W. Lavrijsen, A. Tudor, J. Müller, C. Iancu, and W. De Jong, Classical optimizers for noisy intermediate-scale quantum devices, in *2020 IEEE international conference on quantum computing and engineering (QCE)*, IEEE, 2020, pp. 267–277.
91 R. D'Cunha, T. D. Crawford, M. Motta and J. E. Rice, Challenges in the use of quantum computing hardware-efficient ansaetze in electronic structure theory, *J. Phys. Chem. A*, 2023, **127**, 3437.
92 D. W. Berry, Y. Tong, T. Khattar, A. White, T. I. Kim, S. Boixo, L. Lin, S. Lee, G. K.-L. Chan, R. Babbush and N. C. Rubin, Rapid initial-state preparation for the quantum simulation of strongly correlated molecules, *PRX Quantum*, 2025, **6**, 020327.
93 M. Mörchen, G. H. Low, T. Weymuth, H. Liu, M. Troyer and M. Reiher, Classification of electronic structures and state preparation for quantum computation of reaction chemistry, *arXiv*, 2024, preprint, arXiv:2409.08910, DOI: **10.48550/arXiv.2409.08910**.
94 P. J. Ollitrault, C. L. Cortes, J. F. Gonthier, R. M. Parrish, D. Rocca, G.-L. Anselmetti, M. Degroote, N. Moll, R. Santagati and M. Streif, Enhancing initial state overlap through orbital optimization for faster molecular electronic ground-state energy estimation, *arXiv*, 2024, preprint, arXiv:2404.08565, DOI: **10.48550/arXiv.2404.08565**.
95 H. G. A. Burton, D. Marti-Dafcik, D. P. Tew and D. J. Wales, Exact electronic states with shallow quantum circuits from global optimisation, *Npj Quantum Inf.*, 2023, **9**, 75.
96 K. Sugisaki, S. Yamamoto, S. Nakazawa, K. Toyota, K. Sato, D. Shiomi and T. Takui, Open shell electronic state calculations on quantum computers: A quantum circuit for the preparation of configuration state functions based on serber construction, *Chem. Phys. Lett.*, 2019, **737**, 100002.
97 K. Sugisaki, S. Yamamoto, S. Nakazawa, K. Toyota, K. Sato, D. Shiomi and T. Takui, Quantum chemistry on quantum computers: A polynomial-time quantum algorithm for constructing the wave functions of open-shell molecules, *J. Phys. Chem. A*, 2016, **120**, 6459–6466.
98 A. Carbone, D. E. Galli, M. Motta and B. Jones, Quantum circuits for the preparation of spin eigenfunctions on quantum computers, *Symmetry*, 2022, **14**, 624.
99 D. Marti-Dafcik, H. G. A. Burton, and D. P. Tew, Spin coupling is all you need: Encoding strong electron correlation on quantum computers, *arXiv*, 2024, preprint, arXiv: 2404.18878.
100 P. J. Ollitrault, C. L. Cortes, J. F. Gonthier, R. M. Parrish, D. Rocca, G.-L. Anselmetti, M. Degroote, N. Moll, R. Santagati and M. Streif, Enhancing initial state overlap through orbital optimization for faster molecular electronic ground-state energy estimation, *Phys. Rev. Lett.*, 2024, **133**, 250601.
101 G. Li Manni, W. Dobrautz and A. Alavi, Compression of spin-adapted multiconfigurational wave functions in exchange-coupled polynuclear spin systems, *J. Chem. Theory Comput.*, 2020, **16**, 2202–2215.
102 G. Li Manni, W. Dobrautz, N. A. Bogdanov, K. Guther and A. Alavi, Resolution of low-energy states in spin-exchange transition-metal clusters: Case study of singlet states in [fe(iii)4s4] cubanes, *J. Phys. Chem. A*, 2021, **125**, 4727–4740.
103 W. Dobrautz, V. M. Katukuri, N. A. Bogdanov, D. Kats, G. Li Manni and A. Alavi, Combined unitary and symmetric group approach applied to low-dimensional heisenberg spin systems, *Phys. Rev. B*, 2022, **105**, 195123.
104 L. Kong, F. A. Bischoff and E. F. Valeev, Explicitly correlated r12/f12 methods for electronic structure, *Chem. Rev.*, 2011, **112**, 75–107.
105 A. Grüneis, S. Hirata, Y.-y. Ohnishi and S. Ten-no, Perspective: Explicitly correlated electronic structure theory for complex systems, *J. Chem. Phys.*, 2017, **146**, 080901.
106 C. Hättig, W. Klopper, A. Köhn and D. P. Tew, Explicitly correlated electrons in molecules, *Chem. Rev.*, 2011, **112**, 4–74.
107 P. Schleich, J. S. Kottmann and A. Aspuru-Guzik, Improving the accuracy of the variational quantum eigensolver for molecular systems by the explicitly-correlated perturbative [2]r12-correction, *Phys. Chem. Chem. Phys.*, 2022, **24**, 13550–13564.
108 H. Volkmann, R. Sathyanarayanan, A. Saenz, K. Jansen and S. Kühn, Chemically accurate potential curves for h2 molecules using explicitly correlated qubit-adapt, *J. Chem. Theory Comput.*, 2024, **20**, 1244–1251.
109 S. F. Boys and N. C. Handy, A calculation for the energies and wavefunctions for states of neon with full electronic correlation accuracy, *Proc. R. Soc. London, Ser. A*, 1969, **310**, 63.
110 A. J. Cohen, H. Luo, K. Guther, W. Dobrautz, D. P. Tew and A. Alavi, Similarity transformation of the electronic schrödinger equation via jastrow factorization, *J. Chem. Phys.*, 2019, **151**, 061101.
111 J. P. Haupt, S. M. Hosseini, P. López Ríos, W. Dobrautz, A. Cohen and A. Alavi, Optimizing jastrow factors for the transcorrelated method, *J. Chem. Phys.*, 2023, **158**, 224105.

112 W. Dobrautz, A. J. Cohen, A. Alavi and E. Giner, Performance of a one-parameter correlation factor for transcorrelation: Study on a series of second row atomic and molecular systems, *J. Chem. Phys.*, 2022, **156**, 234108.
113 W. Dobrautz, H. Luo and A. Alavi, Compact numerical solutions to the two-dimensional repulsive hubbard model obtained via nonunitary similarity transformations, *Phys. Rev. B*, 2019, **99**, 075119.
114 M. Motta, T. P. Gujarati, J. E. Rice, A. Kumar, C. Masteran, J. A. Latone, E. Lee, E. F. Valeev and T. Y. Takeshita, Quantum simulation of electronic structure with a transcorrelated hamiltonian: improved accuracy with a smaller footprint on the quantum computer, *Phys. Chem. Chem. Phys.*, 2020, **22**, 24270–24281.
115 S. McArdle and D. P. Tew, Improving the accuracy of quantum computational chemistry using the transcorrelated method, *arXiv*, 2020, preprint, arXiv:2006.11181, DOI: **10.48550/arXiv.2006.11181**.
116 A. Kumar, A. Asthana, C. Masteran, E. F. Valeev, Y. Zhang, L. Cincio, S. Tretiak and P. A. Dub, Quantum simulation of molecular electronic states with a transcorrelated hamiltonian: Higher accuracy with fewer qubits, *J. Chem. Theory Comput.*, 2022, **18**, 5312–5324.
117 H. G. A. Burton, Tiled unitary product states for strongly correlated hamiltonians, *Faraday Discuss.*, 2024, **254**, 157–169.
118 J. S. Kottmann and A. Aspuru-Guzik, Optimized low-depth quantum circuits for molecular electronic structure using a separable-pair approximation, *Phys. Rev. A*, 2022, **105**, 032449.
119 J. S. Kottmann, Molecular quantum circuit design: A graph-based approach, *Quantum*, 2023, **7**, 1073.
120 M. H. Cheng, K. E. Khosla, C. N. Self, M. Lin, B. X. Li, A. C. Medina and M. S. Kim, Clifford circuit initialisation for variational quantum algorithms, *Phys. Rev. A*, 2025, **111**, 062413.
121 Z.-X. Shang, M.-C. Chen, X. Yuan, C.-Y. Lu and J.-W. Pan, Schrödinger-heisenberg variational quantum algorithms, *Phys. Rev. Lett.*, 2023, **131**, 060406.
122 E. Magnusson, A. Fitzpatrick, S. Knecht, M. Rahm and W. Dobrautz, Towards efficient quantum computing for quantum chemistry: Reducing circuit complexity with transcorrelated and adaptive ansatz techniques, *Faraday Discuss.*, 2024, **254**, 402–428.
123 S. Patil, D. Mondal, and R. Maitra, Machine learning approach towards quantum error mitigation for accurate molecular energetics, *arXiv*, 2020, preprint, arXiv:2504.07077, DOI: **10.48550/arXiv.2504.07077**.
124 M. Maronese, L. Moro, L. Rocutto, and E. Prati, Quantum compiling, *arXiv*, 2021, preprint, DOI: **10.48550/arXiv.2112.00187**.
125 H. Safi, M. Bandic, C. Niedermeier, C. G. Almudever, S. Feld, and W. Mauerer, Stacking the odds: Full-stack quantum system design space exploration, *arXiv*, 2025, preprint, arXiv:2506.02782, DOI: **10.48550/arXiv.2506.02782**.
126 H. Zou, Repository for: Multireference error mitigation for quantum computation of chemistry, 2025, **https://zenodo.org/records/15827822**.